JOURNAL OF SPACECRAFT AND ROCKETS
Vol. 37, No. 2, March–April 2000

Current Collection Model Characterizing Shuttle Charging During the Tethered Satellite System Missions

Victor M. Agüero*
SRI International, Menlo Park, California 94025
Brian E. Gilchrist†
University of Michigan, Ann Arbor, Michigan 48109-2134
Scott D. Williams‡
Stanford University, Stanford, California 94305
William J. Burke§
U.S. Air Force Research Laboratory, Hanscom Air Force Base, Massachusetts 01731-3010
and
Linda Krause¶ and Louise C. Gentile**
Boston College, Chestnut Hill, Massachusetts 02467-3862

This research presents a new mathematical model characterizing the negative potential electrical charging behavior of large spacecraft in low Earth orbit that are actively collecting charge, such as part of an electrodynamic tether system. The analysis was carried out to identify significant plasma current sources affecting steady-state spacecraft charging using data from the tethered satellite system missions. During both tethered satellite missions (Aug. 1992 and Feb. 1996), Space Shuttle Orbiter charging was lower than expected. The current collected by the Orbiter greatly exceeded premission predictions based on thin sheath, ram-dominated current collection. Our investigation revealed that the tethered satellite deployer boom was conducting and was grounded to the Orbiter providing a significant current path from the plasma. Modeling results suggest that the plasma sheath significantly augmented the ram current collected by the main engine nozzles and the satellite deployer boom by expanding the effective current collecting area.

Nomenclature

A_y = area associated with surface y, m^2
i_{tether} = tether current, A
j_B = Bohm-corrected flux across the sheath edge, A m^{-2}
$j_{\text{ram},i}$ = ram ion current flux, A m^{-2}
$j_{\text{therm},y}$ = thermal current flux for species y, A m^{-2}
m_i = ion mass (O^+), 2.678×10^{-26}, kg
n_y = particle density of species y, m^{-3}
q = electron charge, 1.602×10^{-19}, C
R_T = total resistance of the tether R_{tether} and loads R_{load} in the circuit, Ω
r_y = radius of object y, m
t_{sh} = sheath thickness, m
v_y = thermal velocity of species y, m s^{-1}
V_{TVMDC} = measured tether voltage, V
v_{orb} = relative velocity between the Orbiter and ambient plasma, ~7300, m s^{-1}
Γ_{sh} = thermal current flux j_{therm} at the sheath edge (i.e., where $n_i = n_{i,\text{sheath}}$), A m^{-2}
ϵ_0 = permittivity of free space, 8.854×10^{-12}, F m^{-1}
ϕ_{EMF} = plasma potential difference between tether endpoints, V
ϕ_{orb} = orbiter potential with respect to local plasma, V
ϕ_{sat} = satellite potential with respect to local plasma, V

Subscripts

i, e = O^+ ions and electrons

Introduction

NASA'S proposal to use large low-Earth-orbit (LEO) spacecraft as science and engineering experiment platforms motivated the need to understand and characterize the electrical charging and current collection of the Space Shuttle Orbiter and the International Space Station. This study evaluated the negative potential electrical charging response of the Orbiter and the resulting current collection. The approach was empirical in nature because of "the lack of reliable quantitative predictions prior to the TSS-1 mission."[1] We present a new model for current collection by the Space Shuttle Orbiter derived from an analysis of tether voltage and current measurements made during the tethered satellite system (TSS) missions. Discrepancies between these measurements and the charging induced potentials predicted prior to flight were used to develop the new current collection model that closely matched the mission results.

Although the study of spacecraft charging to date has resulted in well-defined criteria for engineering design and has aided scientific data interpretation, there remains significant unpredictability in spacecraft electrical response when the knowledge is applied to specific spacecraft.[2–5] Furthermore, the electric potential of large spacecraft such as the Orbiter and the proposed space station can be affected by complicated external and internal phenomena. Ambient plasma flow disturbances as well as spacecraft surface materials and geometries present significant challenges in predicting the electrical response of large spacecraft.[5,6] Even the measurement of spacecraft potential remains inherently difficult and requires careful attention to 1) the references with respect to which potential is measured, 2) the effects of the spacecraft attitude and probes on measurements, and 3) the presence of specific materials and differential charging.

Received 16 October 1998; revision received 19 May 1999; accepted for publication 12 June 1999.

*Research Engineer, Applied Electromagnetics Laboratory (MS 408-95), 333 Ravenswood Avenue. Member AIAA.
†Associate Professor of Electrical Engineering and Space Sciences, 2455 Hayward Avenue. Senior Member AIAA.
‡Research and Development Engineer, W. W. Hansen Experimental Physics Laboratory. Member AIAA.
§Senior Research Physicist, 29 Randolph Road.
¶Research Scientist, Institute for Scientific Research, 402 St. Clement's Hall, 140 Commonwealth Avenue.
**Research Analyst, Institute for Scientific Research, 402 St. Clement's Hall, 140 Commonwealth Avenue.

Consequently, spacecraft charging analysis techniques have evolved incrementally with careful iterations between theory, simulations, and experiments.

The TSS missions provided perfect opportunities to address steady-state charging of the Orbiter using active collection of plasma current and a tethered satellite as a remote plasma potential reference. Previous studies of spacecraft charging lacked such an undisturbed or reliable plasma potential reference. TSS precursor flights had investigated system issues, instrumentation, and the physics of tether-plasma interactions.[7] The TSS missions were reviewed preflight,[8] and the instrumentation and scientific goals have been described comprehensively.[8–10]

This paper presents the results of this study and extends dissertation research pursued by one of the authors during the TSS project.[11] The experiment and methodology used to analyze Orbiter charging are described, and comparisons between measured data, premission models, and a new postmission current collection model are presented. The analysis used in developing the new Orbiter current collection model is discussed.

Experiment Description and Measurements

The TSS missions were launched on 31 July 1992 (TSS-1) and 22 February 1996 (TSS-1R) and flew in 300-km circular orbits at a 28.5-deg inclination. During TSS-1 (TSS-1R), an electrically conductive, 1.6-m diam satellite was deployed to a distance of 268 m (19.7 km) above the payload bay of the Space Shuttle Orbiter *Atlantis* (*Columbia*). The satellite was connected to the Orbiter via an electrically conducting insulated tether. The eastward orbital motion of this system through the geomagnetic field induced an emf that could drive current along the tether and that resulted in currents up to ~30 mA during TSS-1 and 1.1 A during TSS-1R. The Orbiter charged negatively to potentials with respect to the ambient plasma of up to ~−60 V and −600 V, respectively.[12,13]

Tether current and potential differences between the tether and Orbiter were recorded by the shuttle electrodynamic tether system (SETS) with the tether current and voltage monitor (TCVM) located in the payload bay of the Orbiter. The TCVM made highly accurate measurements of the induced potential using the tether voltage monitor (TVMDC), a high-impedance, low-pass filtered (128 Hz) voltmeter. During TSS-1, TVMDC was sampled with 16-bit resolution at 360 Hz and averaged to 24 Hz. On TSS-1R, the sampling rate was reduced to 192 Hz but otherwise remained the same. Tether current could be modified by switching various resistive loads into the circuit and was measured using the TCVM's tether current monitor (TCM), a Hall effect current sensor, sampled with 16-bit resolution at 24 Hz, and through which the tether itself was routed. A full description of the SETS experiment and operations is given by Aguero et al.[14]

For the analysis of TSS-1R data, potentials measured by the Shuttle Potential and Return Experiment (SPREE) were also used to verify predicted Orbiter potentials. The core elements of SPREE are two nested, triquadraspherical electrostatic analyzers (ESAs) that simultaneously recorded fluxes of electrons and ions with energies between 10 eV and 10 keV over a 100×8.5 deg angular fan.[15] Spectra were taken at a rate of 8 s^{-1} in 32 channels logarithmically spaced in energy. The 100-deg dimension of the angular fan was divided into 10 zones of 10 deg width, designated 0 through 9. Ion and electron spectra were measured independently in each zone. Zone 0 had its lower edge 5 deg below parallel to the base of the ESA units, while zone 9 looked 5 deg beyond orbiter zenith. The ESAs, designated A and B, were mounted on rotary tables that turned 6 deg s^{-1} and were synchronized so that both ion and electron spectra were sampled over a solid angle of 2π sr every 30 s. To ensure unsaturated measurements during electron beam operations, the geometric factor of ESA B was set ~100 times smaller than that of ESA A. Because the data in this study do not involve electron beam operations, we use only data from ESA A. The aperture planes of both sensors were grounded to the orbiter frame. The orbiter's potential ϕ_{orb}, with respect to the local plasma, was determined from spectral peaks in ion fluxes measured by SPREE.[12] When the satellite potential ϕ_{sat}, with respect to the local plasma was measured, the orbiter potential inferred from Ohm's law agrees with SPREE determined values to within measurement uncertainties.[13,16]

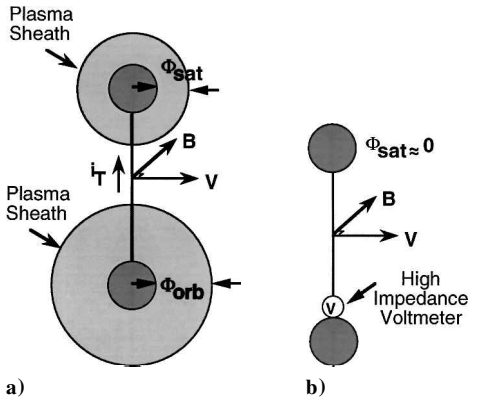

Fig. 1 Schematic representation of a) TSS low-impedance mode of operation and b) TSS high-impedance mode of operation.

Orbiter charging could be studied in either a low- or a high-impedance mode. In the low-impedance mode electrical contact between the tether and the end bodies allowed the available emf to drive a current in the tether and between the plasma and end bodies. In this mode, depicted in Fig. 1a, the satellite collected electrons from the ionosphere, which were driven down the tether and balanced by current collection at the Orbiter. Current flowed through a load resistor within the TCVM to the Orbiter frame. In high-impedance mode the tether remained electrically isolated by a high-impedance load placed between the tether and the Orbiter. The satellite served as a reference potential from which the induced tether voltage was measured using the TVMDC circuit as a high-impedance voltmeter as depicted in Fig. 1b. The system then allowed negligible tether current flow, and each of the spacecraft was approximately at its local plasma potential.[17,18] The resulting voltmeter output was a sum of the potential induced by the motional emf, any offsets caused by charging, and any superimposed ionospheric electric fields.[11,18–21]

Data acquired during the low-impedance operating mode were selected for this study because of the high potentials that resulted from the flow of tether current. At the Orbiter tether current was balanced either by the collection of positive ions from the ionosphere (predominantly O^+ ions), the emission of electron beams from electron guns on the Orbiter, or secondary electron emission caused by ion impingement on Orbiter conducting surfaces. During most of the deployed phase of both TSS missions, the Orbiter was oriented with its largest conducting surfaces, the main engine nozzles, facing the ram direction. When electron guns were not firing, Orbiter charging occurred when the ram ion flux was smaller than the tether current.

Orbiter electrical potential was computed from the tether current and voltage measurements. Accurate knowledge of the induced emf, the tether potential drop, satellite potential, and other voltage-inducing effects makes it possible to compute the Orbiter potential by solving for the TSS circuit potential distribution. In the dc mode of operation, the TSS circuit can be reduced to a relatively simple equivalent circuit that replaces the complexity of the electrical response at each endpoint of the system by a voltage-controlled current source (cf. Fig. 1). Potential distribution in the system while operating in this mode and assuming ion current collection by the main engine bells was addressed.[17] The ionospheric impedance associated with the plasma contact at each end body had previously been considered and was found to be negligible.[22,23]

Treating the complex endpoint plasma contacts as nonlinear current sources, it is possible to write a simple circuit equation for the system. The result is described by Ohm's law involving the sum of the voltages around a closed circuit. Assuming negligible ionospheric impedance and negligible ambient electric fields (typically smaller than 5 mV/m),[21] the equation is

$$-\phi_{\text{orb}} - \phi_{\text{EMF}} + i_{\text{tether}} R_T + \phi_{\text{sat}} = 0 \tag{1}$$

where $R_T = R_{\text{tether}} + R_{\text{load}}$ represents the total resistance of the tether and loads in the circuit. The polarity of the current sources has been

chosen such that, when their voltages are positive, electrons are attracted from the plasma (or ions move to the plasma).

The Orbiter negative potential can be quantified by using the measured tether current i_{tether} and voltage V_{TVMDC}. With the substitution $V_{\text{TVMDC}} = -\phi_{\text{EMF}}$, Eq. (1) can be rearranged to give the equation

$$\phi_{\text{orb}} = V_{\text{TVMDC}} + i_{\text{tether}} R_T + \phi_{\text{sat}} \tag{2}$$

The motionally induced emf was determined by a linear interpolation across data from high-impedance periods (negligible current flow) surrounding intervals of tether current flow. This approach leads to small errors as a result of the slowly varying nature of the motionally induced emf and the low level of other voltage noise sources such as naturally occurring ionospheric electric fields.[11,14,19–21]

The value for R_T used for TSS-1 was 2.0 kΩ and for TSS-1R estimated at 1.8 kΩ (Refs. 16 and 24). The greatest cause of variation in the tether resistance between TSS-1 and TSS-1R resulted from the variation with temperature of 8 Ω/°C. The 2.0 kΩ value used for TSS-1 data analysis is within 3% of the maximum and minimum expected because the TSS-1 tether remained mostly on the tether reel and in a well-controlled temperature range within the Orbiter payload bay.[25] The value of 1.8 kΩ used for TSS-1R is an average of the value encountered with short deployments and the smallest TSS-1R value resulting from cold operations at full deployment. For any given TSS-1R charging event, the resistance variation was mostly driven by temperature differences between day and night periods, and the 1.8 kΩ value lies within 10–13% of the extremes determined from measurements of tether current and voltage.[26]

For the TSS-1 deployment of 268 m, the tether current rarely became large compared to the satellite thermal current, and thus $\phi_{\text{sat}} \approx 0$ (Refs. 14 and 27). Consequently, the satellite generally collected whatever current could be balanced at the Orbiter end of the system. For the TSS-1R data used in this study, satellite potential was measured with a satellite-based Langmuir probe,[28] and SPREE measurements of Orbiter potentials were compared with Orbiter potentials computed from tether measurements.[13,16] Data were also selected for events with 1) no active electron gun operations, 2) no thruster firings or significant perturbations from Orbiter activity such as water dumps, and 3) available plasma density measurements. Satisfying these criteria eliminated more than half of the TSS-1 negative charging events. The greatest limitation was the intermittent measurements of plasma density, which in many cases left undetermined a primary independent variable affecting Orbiter charging. Events involving electron gun and thruster firings were not considered because of the ambiguity in specifying how these activities affected current collection.[29]

Before attempting to understand current collection by the Orbiter, it is useful to establish that the charging data are consistent with Ohm's law. Figure 2 shows a plot of the inferred Orbiter potential vs density for the TSS-1 data used initially to derive the model described in this paper. The charging induced Orbiter potential has greater magnitude at lower density, as expected, because at lower densities greater electrical potential is needed to collect the ions balancing the tether current arriving at the Orbiter. At high densities the potential remains low because the ram ion flux equals or exceeds the tether current. In addition, the potential for each point plotted in Fig. 2 has a smaller magnitude than the emf across the system.[11] The Orbiter potential being less than the emf available is consistent with the fact that the emf is distributed across the tether and sheath drops and represents an upper bound on possible charging induced potential when no electron guns were firing.

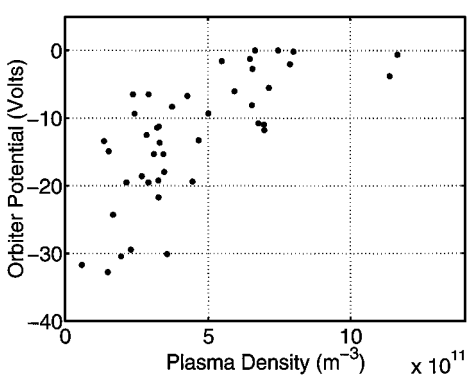

Fig. 2 Inferred Orbiter potential vs the plasma density during TSS-1.

Analysis and Results

Prior to the TSS missions, it was believed the tether current in the simple operating modes and over the range of orbiter potentials discussed here would be approximately equal to the Orbiter's ram current collection.[17] Because of the Orbiter's limited ability to collect ion current, i_{tether} would be small and most of ϕ_{EMF} would appear as high values of ϕ_{orb}. Data from TSS-1 disproved this conjecture and motivated this new study of current collection at the Orbiter to determine how the measured tether current was balanced. This analysis was carried out in three steps: 1) TSS-1 measured currents were compared against predictions from the premission models, 2) a new numerical model for Orbiter current collection was developed to resolve discrepancies between measured and modeled tether currents, and 3) new model predictions were compared with TSS-1R measurements.

Pre-TSS Models

Although specific examples of negative Orbiter charging have been documented,[14,19,20] an attempt to characterize Orbiter charging using TSS-1 data was only recently presented.[11] Because of the mesosonic nature of the Orbiter's motion with respect to the plasma, the ram ion current was identified as the primary source balancing the tether current[17] and was collected by an effective area of ~25 m^2 (Refs. 19 and 30). Consequently, pre-TSS-1 models were based on the assumption that ion collection at the Orbiter was dominated by the ram ion contribution.[19,30] Prior missions dealt primarily with electron collection. Effective collecting areas derived from those results did not apply to ion collection under negative charging conditions.[31]

This effective collection-area model assumed that ion collection would not be enhanced significantly by the low magnitude potentials encountered during TSS-1. Hence, the collecting area remained fixed over the entire range of potentials used in this study. This area was, in fact, larger than the ram projected area of the Orbiter's main engine nozzles, which is 15.3 m^2 (Ref. 11). As a result, this approach underpredicts current collection at higher potentials and overpredicts at lower potentials. The assumption of negligible current collection increase with increased electrical potential is not accurate even at the level of tens of volts encountered during TSS-1. A model was needed that reflected the observed current collection increase with increasing charging induced potentials.

A-96 Model Development

Increased current collection with increasing potential showed a trend similar to that expected for a growing sheath. Thus a new model must allow for a plasma sheath that increased the effective collecting area.[1] Figure 3 shows a schematic representation of the sheath structure around an Orbiter engine nozzle. Ram ions entering the sheath are collected as a result of their trajectories being deflected by the sheath attractive potential. A consideration of the sheath thickness at higher spacecraft potential and the separation between main engine nozzles of (~0.2 m) suggested that a simple computation would overpredict the collecting area as a result of

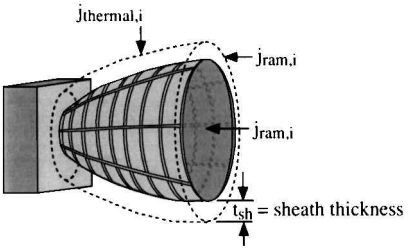

Fig. 3 Schematic representation of the sheath structure around an Orbiter engine nozzle.

sheath overlaps. In fact, not accounting for the overlap results in an effective current collecting area that increases at a rate even faster than that observed in the TSS-1 data. Successful modeling thus required an accurate area calculation avoiding the multiple counting of overlapping sheath regions around the engine nozzles.

Although the trend shown by the sheath-augmented model was closer to the measurements than fixed area models, the predicted currents still did not grow at observed rates. This exercise demonstrated, first, that at potentials less than ~ -5 V, the collecting area was ~ 15.3 m^2. At low Orbiter potentials sheath thickness remained small compared to the size of the main engine nozzles and contributed little added current collection. Second, the sheath thickness grew as the Orbiter potential rose to increase current collection. However, accounting for engine nozzle sheaths alone did not increase current collection at a rate comparable to that shown in the data. The model must account for additional current collection but not contradict the low-potential ram collecting area of the engine nozzles, ~ 15.3 m^2.

These discrepancies led to a reevaluation of the assumptions about Orbiter current collecting areas and sheath growth. Mechanisms that increase ion current collection but do not add additional ram projected area include thermal collection to other conducting surfaces on the Orbiter, photoemission, and impact ionization. Of these, all but thermal collection were ruled out because of the low yields at TSS-1 velocities and charging levels.[3] Two possible thermal collection issues were considered: 1) the magnitude of the thermal collection contribution to the engine nozzles and 2) the possible existence of additional current collecting areas.

The ion thermal current contribution remains quite small because the thermal flux is only about 4% of the ram flux to a given surface area, that is, $j_{\text{therm},i} = \frac{1}{4} n_i \overline{|v_i|} q$ is only 4% of $j_{\text{ram},i} = n_i v_{\text{orb}} q$, or $j_{\text{therm},i} / j_{\text{ram},i} \approx 0.04$. As a result, even though the nozzle exterior surface area of ~ 54.5 m^2 is larger than the ram projected nozzle area of ~ 15.3 m^2, the area ratio $A_{\text{therm}} / A_{\text{ram}} \approx 3.56$ results in the thermal flux contributing less than 15% of the total current collected. Careful study of the Orbiter revealed only a few square meters of conducting surface (payload bay vent grills, small thruster nozzles, and conducting payload blankets) that were not included in the premission models.[11] Hence, the thermal contribution to the current balance could never be comparable to the ram contribution nor account for the large increase in collection area shown by the TSS-1 data at the higher Orbiter potentials.

This remaining discrepancy between the modeled and observed current collection led to the discovery that the satellite deployer boom had a number of exposed conducting surfaces. Figure 4 shows the deployer boom during testing. During the missions, this structure protruded radially outward from the shuttle payload bay approximately 12 m. The width of the boom lattice is ~ 0.45 m, whereas the longerons themselves are ~ 1 cm thick. The vertical longerons of ~ 11.5 m length are aluminum with a conducting irridite surface.

Fig. 4 Satellite deployer boom assembly during a ground test. The boom is a space lattice structure consisting of vertical aluminum longerons and various battens interconnecting the longerons for support and was mounted on the pallet installed in the Orbiter payload bay. (Courtesy of AEC Able Engineering.)

The diagonal elements in the lattice are conducting steel tension wires. The horizontal battens that divide the boom into bays alternate between conducting aluminum and nonconducting fiberglass. These battens are attached to the longerons with aluminum fittings at slip joints using steel pins. Discussion in 1995 and 1996 with the contractor responsible for the deployment subsystem suggested that a conducting path existed along the full length of the boom to Orbiter ground. This had been overlooked in conducting material assessments because the boom contained a significant number of nonconducting elements and a grounding strap that ran down the inside of the boom between the top end (known as the Tip Can) and the lower deployer mechanism. The ground strap was there to meet ground-path electrical specification requirements, not to ensure a conducting path. Tests performed after the TSS-1R mission provided a deployer boom tip can to Orbiter resistance of $\sim 33\ \Omega$.

This discovery suggested that the deployer boom provided the missing current collecting surface with characteristics consistent with the conclusion that the main engine nozzles dominated collection by ram-facing conducting area. The boom structure added negligible ram collecting area at very low potential, yet provided a large surface along which a sheath could augment current collection as the charging induced potential increased in magnitude. Because of its lattice structure, the boom contribution to the ram-projected conducting area was a mere ~ 0.2 m^2. However, as the sheath thickness increased, the effective current collecting area of the boom would have increased rapidly because of the long conducting surfaces along which the sheath could develop.

Approximately 9 m of the 12-m boom length were exposed to ram plasma flow, providing a conducting frame with an edge of ~ 18 m along which a sheath could develop. The boom edge represented a conducting surface even longer than the combined nozzle end circumferences of the main engines, which totaled ~ 15 m. This does not include the boom interior, which at low charging magnitudes fills as the sheath grows and adds an additional, but smaller contribution to the effective collecting area. Hence, while adding negligible ram collecting area, the sheath-augmented collecting area represented by the boom longerons was ~ 1.2 times that represented by the main engine bells, and over the range of TSS-1 charging levels was a faster growing contribution to the collecting area than the main engine nozzle sheaths.

An improved collection model incorporating these measurements was developed (referred to as A-96) that showed marked improvement in matching the TSS-1 tether currents.[11] The A-96 current collection model accounts for ram, sheath, and thermal currents to conductors and avoids multiple counting in the overlapping sheath regions between boom lattice members and between the Orbiter's main engine nozzles. The boom sheath collection more than doubled the effective current collection area for the higher TSS-1 Orbiter potentials. Furthermore, the total thermal current contribution included in A-96 added another 15%. The resulting conclusion was that a sheath dependence involving contributions from the boom and nozzles (i.e., $A_{\text{boom,sh}}$ and A_{nozzles}) accounted for the majority of the ion current collection.

The main contributions to the ram-projected current collecting area in A-96 are defined by the equation

$$A_{\text{ram}} = A_{\text{nozzles}} + A_{\text{boom,ram}} + A_{\text{boom,sh}} \tag{3}$$

where $A_{\text{boom,ram}} = 0.2$ m^2, $A_{\text{boom,sh}} = 18 t_{\text{sh}}$, and A_{nozzles} is given by an expression for the nozzle sheath area that does not count overlapping sheath regions. The expression for the ram projected nozzle area is

$$A_{\text{nozzles}} = 3 \times \pi (r_m + t_{\text{sh}})^2 + 2 \times \pi (r_o + t_{\text{sh}})^2 - A_{\text{overlap}} \tag{4}$$

where r_m and r_o are the three space shuttle main engine (SSME) and two orbital maneuvering system (OMS) engine nozzle radii and t_{sh} is the sheath thickness. Details of this overlap area computation are provided in Aguero (whereas simple geometry, the accurate calculation, requires multiple pages to describe).[11]

The equation defining the sheath thickness t_{sh} is

$$t_{\text{sh}} = \tfrac{2}{3} \sqrt{(2/qm_i)^{\frac{1}{2}} \left(\epsilon_0 V^{\frac{3}{2}} / j_B \right)} \tag{5}$$

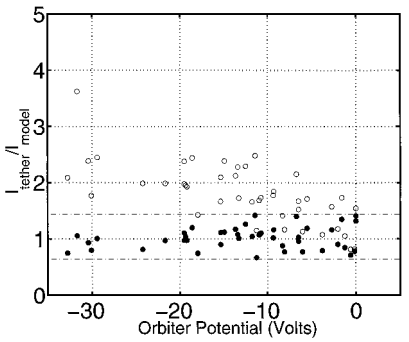

Fig. 5 Ratios of TSS-1 tether current normalized by A-96 predictions (•) and Orbiter ram current (○). Measurement uncertainty is bounded by the dashed line.

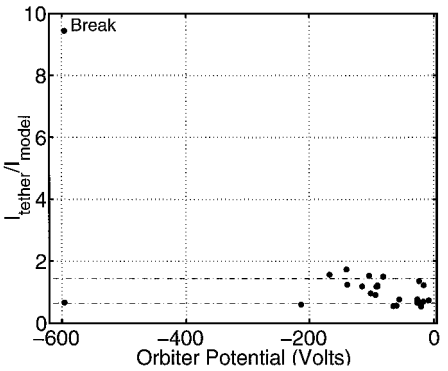

Fig. 6 Ratios of TSS-1R tether current normalized by A-96 predictions.

where $V = |\phi_{\text{orb}}|$ and $j_B = 1.53\Gamma_{\text{sh}}$ is the Bohm-corrected thermal flux across the sheath edge (Ref. 11, Appendix A). The conducting surfaces included in A-96 are the Orbiter engine nozzles, payload bay vent-grills, payload bay conducting blankets, and payload conducting surfaces. In the TSS-1 Orbiter attitude these yield ~ 16 m^2 of the conducting surface exposed to the ram currents and ~ 62 m^2 of the conducting surfaces exposed to thermal currents. The basic model assumptions are that 1) all ram ions entering sheaths are collected, 2) at low-charging magnitudes secondary emissions are not significant, and 3) photoemission current density $\sim 10^{-5}$ A/m^2 contributes negligibly to the daytime current balance compared to measured tether currents.[11,12]

Figure 5 shows two representations of tether currents measured during TSS-1 plotted as a function of ϕ_{orb}. The upper set of points, represented by open circles, shows measured tether currents normalized by ram currents to the Orbiter[11] using the 15.3 m^2 ram-projected nozzle area. These points show that current collection at higher potential magnitudes was up to 3.5 times larger than the simply computed ram current levels. The lower set of points shows the measured tether currents normalized by the A-96 predictions for currents to the Orbiter. Whereas deviations from a ratio of 1 remain between the A-96 predictions and the measured tether currents, these were found to be uncorrelated with other variables or mission operations. The dashed lines in Fig. 5 represent the maximum range that results from an estimated ±20% uncertainty in measured plasma densities.[32]

A-96 Model Comparisons to TSS-1R Data

To compare TSS-1R data with A-96 predictions, a simple cosine projection of the conducting area to the ram direction was adopted to compensate for Orbiter pitch variations of up to 40 deg that occurred during TSS-1R. The Orbiter pitch-induced shadowing of payload-bay conductors from the ram plasma flow was also accounted for by a cosine projection into the payload bay of the aft payload bay bulkhead. This adjustment proved necessary because the Orbiter pitch could reduce the projected sheaths and conducting areas by as much as 20%.

To extrapolate to higher charging induced potentials than achieved during TSS-1, the equation provided by Parker's analytic fit to the Bohm-corrected Child–Langmuir sheath thickness is used.[33] {Parker's result is an analytic fit between the Child–Langmuir flat plate and spherical sheath results allowing extrapolation to sheath thickness values greater than would be justified with only the flat-plate result. Parker's analytic fit is given by the equation

$$t_{\text{sh}} = r_0\left[\tfrac{1}{2} + \sqrt{\tfrac{1}{4} + t_0/r_0} + 0.052(t_0/r_0)H(t_0/r_0 - 0.2)\right] \qquad (6)$$

where r_0 is the radius of the object, t_0 is the sheath thickness as computed using the thermal flux at the sheath edge (Γ_{sh}), and $H(x)$ is the unit step function with $H = 0$ if $x < 0$ and $H = 1$ if $x > 0$. This expression is valid to sheath thicknesses such that $t_0 \leq 19r_0$ (Ref. 33). In the case of the main engine nozzles, using a radius of $r_0 = 1.2$ m, this expression is valid for sheaths less than 22.8 m in thickness.}

Figure 6 shows tether currents measured during TSS-1R plotted as a function of ϕ_{orb}. The data are normalized by the A-96 predictions for currents to the Orbiter using the numerically computed sheath and conducting surface areas already described. At the higher TSS-1R charging levels, the sheath for both nozzles and deployer boom fully encompasses each structure; hence, the boom sheath contributes to sheath area growth at a rate similar to the nozzle sheath. Again, the dominant uncertainty derives from errors in measured plasma densities, as indicated by the dashed lines. A good match is obtained between the model and data at low Orbiter potentials and even with one data point at −600 V. However, the discrepancy between the data and model increases slightly with increasing $|\phi_{\text{orb}}|$. The second data point at −600 V, labeled Break, was taken in the 9 s prior to the tether break when the i_{tether} approached 1 A and $\phi_{\text{orb}} \approx -600$ V (Refs. 13 and 34). At the time of the break, the Orbiter was able to collect >9 times more current than predicted by A-96. This event was unique in TSS operations and involves different current generation physics.[35] The agreement shown in Fig. 6 for the Orbiter current collection extends over a surprisingly large range even though the Orbiter potentials are three to six times those of TSS-1 for which the A-96 model was derived and suggests that space charge limited current collection remains dominant for these charging events.

Conclusions

Our investigation of the Orbiter's ability to collect ion current from the ionosphere validated that tether current and voltage measurements could be used to study spacecraft charging. Data from TSS-1 were found to be adequate for discriminating between plasma current contributions, which explained the lower than expected spacecraft potentials in both TSS missions. This investigation and data analysis lead to the development of an Orbiter ion collection model based on TSS-1 charging data, which improved our ability to predict spacecraft potentials and current collection. The model later demonstrated good agreement with measurements in the much higher magnitude potential regime of TSS-1R.

A review of current collecting surfaces and mechanisms at the Orbiter under conditions of steady-state charging showed that many small conducting surfaces contributed negligibly to the current balance. However, the contribution of even thin sheaths over large surfaces readily enhanced current collection above that by the ram-projected area of the Orbiter's main engine nozzles. The deployer boom was found to be conducting and grounded to the Orbiter. The thin frame of the deployer developed a large area sheath, which even at low TSS-1 charging levels could collect space charge limited currents comparable to those intercepted by the Orbiter main engine nozzles. The combination of current collection from engine nozzle surfaces, the deployer boom lattice, and thin sheaths associated with these surfaces accounted for TSS-1 and TSS-1R observed steady-state tether currents to within the accuracy of the available measurements.

In summary, for large LEO spacecraft having grounded thin-frame lattice structures, ion collection is easier than simple structure models would suggest even at low negative spacecraft potentials. Thin sheaths add significant collecting areas when they develop perpendicular to the ram plasma flow. Thus sheath-augmented ion collection to both large conductors and thin-frame conductors cannot be ignored even for low-charging induced potentials. In particular,

this current collecting ability of thin structures needs to be considered carefully because such structures are expected to form major components of future space stations. Spacecraft potentials depend strongly on geometry and orientation with respect to ram plasma flow. Hence even minor geometry and attitude changes may cause significant changes in charging response.

Acknowledgments

This work was supported in part by NASA and the Tether Program Office at Marshall Space Flight Center under Contracts NAS8-36812 (Stanford University SETS Project) and NAS8-39381 (University of Michigan SETS Project), by the U.S. Air Force Office of Scientific Research Task 2311PL013, and by Air Force Contract F19628-96-K-0030 with Boston College. We are grateful for the data analysis and collaboration with Don C. Thompson and W. John Raitt (also of the SETS Project) at the Center for Atmospheric and Space Science, Utah State University, and for data exchange and discussions from the Research on Electrodynamic Tether Effects (RETE) plasma sensor package provided by the Space Sciences Department (SSD) of ESA/European Space Research and Technology Centre (ESTEC). The RETE DC Boom Package satellite charging and Langmuir Probe plasma density data were contributed by J.-P. Lebreton from the ESA/ESTEC/SSD. Recognition is given to P. M. Banks, D. S. Lauben, P. R. Williamson, and A. B. White for their contributions to the TSS missions. The authors also thank the reviewers of the manuscript.

References

[1]Hawkins, J. G., "Vehicle Charging and Return Current Measurements During Electron Beam Emission Experiments from the Shuttle Orbiter," Ph.D. Dissertation, Dept. of Electrical Engineering, Stanford Univ., Stanford, CA, April 1988.

[2]Samir, U., and Stone, N. H., "Shuttle-Era Experiments in the Area of Plasma Flow Interactions with Bodies in Space," *Acta Astronautica*, Vol. 7, No. 10, 1980, pp. 1091–1141.

[3]Garrett, H. B., "The Charging of Spacecraft Surfaces," *Reviews of Geophysics and Space Physics*, Vol. 19, No. 4, 1981, pp. 577–616.

[4]Laframboise, J. G., and Sonmor, L. J., "Current Collection by Probes and Electrodes in Space Magnetoplasma: A Review," *Journal of Geophysical Research*, Vol. 98, No. A1, 1993, pp. 337–357.

[5]Garrett, H. B., and Whittlesey, A. C., "Spacecraft Charging: An Update," AIAA Paper 96-0143, Jan. 1996.

[6]Hastings, D. E., "A Review of Plasma Interactions with Spacecraft in Low Earth Orbit," *Journal of Geophysical Research*, Vol. 100, No. A8, 1995, pp. 14,457–14,483.

[7]Dobrowolny, M., and Melchioni, E., "Electrodynamics Aspects of the First Tethered Satellite Mission," *Journal of Geophysical Research*, Vol. 98, No. A8, 1993, pp. 13,761–13,778.

[8]Stuart, T., Price, J. M., and Stone, N., "Tethered Satellite System: First Mission Status," AIAA Paper 89-0681, Jan. 1989.

[9]Dobrowolny, M., and Stone, N. H., "A Technical Overview of TSS-1: the First Tethered Satellite System Mission," *Il Nuovo Cimento*, Vol. 17C, No. 1, 1994, pp. 1–12.

[10]Stone, N. H., and Bonifazi, C., "The TSS-1R Mission: Overview and Scientific Context," *Geophysical Research Letters, TSS-1R Special Section: Part 1*, Vol. 25, No. 4, 1998, pp. 409–412.

[11]Aguero, V. M., "A Study of Electrical Charging on Large LEO Spacecraft Using a Tethered Satellite as a Remote Plasma Reference," Ph.D. Dissertation, Dept. of Aeronautics and Astronautics, Stanford Univ., Standford, CA, June 1996.

[12]Machuzak, J. S., Burke, W. J., Gentile, L. C., Davis, V. A., Hardy, D. A., and Huang, C. Y., "Thruster Effects on the Shuttle Potential During TSS 1," *Journal of Geophysical Research*, Vol. 101, No. A6, 1996, pp. 13,437–13,444.

[13]Gentile, L. C., Burke, W. J., Huang, C. Y., Machuzak, J. S., Hardy, D. A., Olson, D. G., Gilchrist, B. E., Lebreton, J.-P., and Bonifazi, C., "Negative Shuttle Charging During TSS-1R," *Geophysical Research Letters*, Vol. 25, No. 4, 1998, pp. 433–436.

[14]Aguero, V. M., Banks, P. M., Gilchrist, B. E., Linscott, I., Raitt, W. J., Thompson, D. C., Tolat, V. V., White, A. B., Williams, S. D., and Williamson, P. R., "The Shuttle Electrodynamic Tether System (SETS) on TSS-1," *Il Nuovo Cimento*, Vol. 17C, No. 1, 1994, pp. 49–65.

[15]Oberhardt, M. R., Hardy, D. A., Slutter, W. E., McGarity, J. O., Sperry, D. J., Everest, A. W., III, Huber, A. C., Pantazis, J. A., and Gough, M. P., "The Shuttle Potential and Return Electron Experiment," *Il Nuovo Cimento*, Vol. 17C, No. 1, 1994, pp. 67–83.

[16]Aguero, V. M., Williams, S. D., Gilchrist, B. E., Habash Krause, L., Thompson, D. C., Raitt, W. J., Burke, W. J., and Gentile, L. C., "Current Collection at the Shuttle Orbiter During TSS-1R High Voltage Charging," *Geophysical Research Letters*, Vol. 25, No. 5, 1998, pp. 729–732.

[17]Banks, P. M., "Review of Electrodynamic Tethers for Space Science," *Journal of Spacecraft and Rockets*, Vol. 26, No. 4, 1989, pp. 234–239.

[18]Williams, S. D., Gilchrist, B. E., Aguero, V. M., Indiresan, R. S., Thompson, D. C., and Raitt, W. J., "TSS-1R Vertical Electric Fields: Long Baseline Measurements Using an Electrodynamic Tether as a Double Probe," *Geophysical Research Letters*, Vol. 25, No. 4, 1998, pp. 445–448.

[19]Thompson, D. C., Raitt, W. J., Bonifazi, C., Williams, S. D., Aguero, V. M., Gilchrist, B. E., and Banks, P. M., "TSS-1: Orbiter Current and Voltage Experiments," AIAA 31st Aerospace Sciences Conf., Jan. 1993.

[20]Williams, S. D., Aguero, V. M., Thompson, D. C., Raitt, W. J., Gilchrist, B. E., Banks, P. M., and Voronka, N. R., "Induced Ionospheric Double Probe Tether Potential Measurements and Models for TSS-1 Electrodynamics," *Proceedings of Fourth International Conference on Tethers in Space*, AIAA, Washington, DC, 1995.

[21]Gilchrist, B. E., Williams, S. D., Voronka, N. R., Raitt, W. J., Thompson, D. C., Bilen, S. G., and Aguero, V. M., "Space Tethers for Double Probe Potential Measurements in the Ionosphere and Magnetosphere," American Geophysical Union, Chapman Conf., April 1995.

[22]Donohue, D. J., "Plasma Wave Radiation Induced by a Conducting Tethered Satellite System," Ph.D. Dissertation, Dept. of Electrical Engineering, Stanford Univ., Stanford, CA, June 1991.

[23]Donohue, D. J., Neubert, T., and Banks, P. M., "Estimated Radiated Power from a Conducting Tethered Satellite System," *Journal of Geophysical Research*, Vol. 96, No. A12, 1991, pp. 21,245–21,253.

[24]Thompson, D. C., Bonifazi, C., Gilchrist, B. E., Williams, S. D., Raitt, W. J., Lebreton, J. P., Vannaroni, G., and Burke, W. J., "The Current-Voltage Characteristics of a Large Probe in Low Earth Orbit: TSS-1R Results," *Geophysical Research Letters*, Vol. 25, No. 4, 1998, pp. 413–416.

[25]Williams, S., "Shuttle Electrodynamic Tether System Instrument Flight Performance Report, SETS-IFPR-01," Dept. of Electrical Engineering, Stanford Univ., Stanford, CA, Aug. 1994.

[26]Chang, C. L., Drobot, A. T., Papadopoulos, K., Wright, K. H., Stone, N. H., Gurgiola, C., Winningham, J. D., and Bonifazi, C., "Current Voltage Characteristics of the Tethered Satellite System: Measurements and Uncertainties due to Temperature Variations," *Geophysical Research Letters*, Vol. 25, No. 5, 1998, pp. 713–716.

[27]Butler, A., Dobrowolny, M., Ekholm, S., Guidoni, U., Harvey, C., Iess, L., Lebreton, J. P., Maggi, M., Melchioni, E., and Vannaroni, G., "RETE Experiment Langmuir Probe Data Analysis for the TSS-1 Mission," Inst. di Fisica dello Spazio Interplanetario, Consiglio Nazionale della Richerche, Rept. IFSI-94-2, Frascati, Italy, 1994.

[28]Dobrowolny, M., Melchioni, E., Guidoni, U., Iess, L., Maggi, M., Orfei, R., deConchy, Y., Harvey, C. C., Manning, R. M., Wouters, F., Lebreton, J. P., Ekholm, S., and Butler, A., "The RETE Experiment for the TSS-1 Mission," *Il Nuovo Cimento*, Vol. 17C, No. 1, 1994, pp. 101–121.

[29]Burke, W. J., Raitt, W. J., Thompson, D. C., Machuzak, J. S., Gentile, L. C., Gilchrist, B. E., Huang, C. Y., Cooke, D. L., Hardy, D. A., Olson, D. G., Lebreton, J.-P., and Bonifazi, C., "Shuttle Charging by Fixed Energy Electron Beam Emissions," *Geophysical Research Letters*, Vol. 25, No. 5, 1998, pp. 725–728.

[30]Oberhardt, M. R., Hardy, D. A., Thompson, D. C., Raitt, W. J., Melchioni, E., Bonifazi, C., and Gough, M. P., "Positive Spacecraft Charging as Measured by the Shuttle Potential and Return Electron Experiment," *IEEE Transactions on Nuclear Science*, Vol. 40, No. 6, 1993, pp. 1532–1541.

[31]Banks, P. M., Raitt, W. J., White, A. B., Bush, R. I., and Williamson, P. R., "Results from the Vehicle Charging and Potential Experiment on STS-3," *Journal of Spacecraft and Rockets*, Vol. 24, No. 2, 1987, pp. 138–149.

[32]Lebreton, J.-P., "Analysis Method of the Langmuir Probe I-V Characteristics (Rev. 1)," ESA/European Space Research and Technology Centre, Space Sciences Dept. Internal Note, Noordwijk, The Netherlands, March 1996.

[33]Parker, L. W., "Plasmasheath-Photosheath Theory for Large High-Voltage Space Structures," *Space Systems and Their Interactions with the Earth's Space Environment*, edited by H. B. Garrett, and C. P. Pike, AIAA, New York, 1980, pp. 477–522.

[34]Gilchrist, B. E., Bonifazi, C., Bilen, S. G., Raitt, W. J., Burke, W. J., Stone, N. H., and Lebreton, J.-P., "Enhanced Electrodynamic Tether Currents due to Electron Emission from a Neutral Gas Discharge: Results from the TSS-1R Mission," *Geophysical Research Letters*, Vol. 25, No. 4, 1998, pp. 437–440.

[35]Aguero, V. M., Burke, W. J., Gilchrist, B. E., Stone, N. H., Gentile, L. C., Williams, S. D., Cooke, D. L., Thompson, D. C., Bonifazi, C., and Lebreton, J.-P., "Current Collection at the Shuttle Orbiter During the Tethered Satellite System Tether Break," *Journal of Geophysical Research*, Vol. 104, No. A1, 1999, pp. 105–114.

I. E. Vas
Associate Editor